

Control of Morphological and Rheological Properties of Carrot Cell Wall Particle Dispersions through Processing

Li Day · Mi Xu · Sofia K. Øiseth · Yacine Hemar · Leif Lundin

Received: 18 December 2009 / Accepted: 19 March 2010 / Published online: 5 May 2010
© Springer Science+Business Media, LLC 2010

Abstract A range of thermal and mechanical processes were used to create dispersions with different particle morphologies, i.e., systems that contain primarily plant cell wall clusters with an average particle size ($d(0.5)$) of ~ 200 μm , single cells ($d(0.5) \sim 70$ μm) or cell fragments ($d(0.5) \sim 40$ μm). The small and large deformation rheology (viscoelastic properties and flow properties) of these dispersions, with a range of total solid contents covering textures varying from a fluid to a paste, were determined. The particle dispersions showed weak gel-like behaviour. Their elastic modulus (G') as a function of total solid content exhibited three regions of different rheological behaviours. The particles formed particulate colloidal networks at relatively low solid content. The interaction of particles contributed to the sharp increase in the elastic modulus of the dispersion in the concentrated region. Further packing of particles beyond the critical packing volume fraction, caused the G' for the 'cluster-cell' and the 'single-cell' dispersions to reach a plateau value. This is due to particle deformation resulting in changes in their microstructure and their ability to pack closely. Plant particle dispersions displayed abrupt yielding at the critical stress with a 3–4 order decrease in viscosity and high yield stress at low solids due to the formation of particulate colloidal network.

Keywords Plant cell wall material · Particle dispersion · Structure · Rheology · Flow properties

Introduction

There is a global trend in the food manufacturing industry towards the development of convenient and good-tasting food with enhanced health benefits. The food industry is investing in Research and Development to find technical solutions to reduce the salt/sugar content, calorific value and to increase the nutritional value of processed food. There is a substantial potential for new foods using plant cell dispersions with healthier compositions and with no added stabilisers or thickeners. Functional plant cell wall particulate materials can offer opportunities to add value to by-products or waste streams from the primary production of fruits and vegetables (Di Giacomo and Taglieri 2009).

A large proportion of foods containing plant-based materials, such as tomato sauce, homogenous vegetable soups and dips, rely on interactions between plant cell particles to impart the desired rheological properties, product texture and related sensory properties. The rheological properties of plant particle dispersions are determined by the particle shape, size and distribution; particle concentration and deformability and hydrodynamic forces arising from the relative motion of particles in the surrounding fluid (Pabst et al. 2006; Genovese et al. 2007; Ortega-Rivas 2009). For example, in a concentrated form such as tomato paste, the viscosity of the system is largely controlled by the deformability of close-packed particles (Yoo and Rao 1994; Valencia et al. 2003). Rheological properties of rehydrated cell wall particles prepared from apple and carrot have also been reported (Vetter and Kunzek 2003; Schalow and Kunzek 2004; Pickardt et al. 2004). In a diluted system, the viscosity is primarily determined by the volume fraction of particle, spatial distance and neighbouring particle interactions (Evans and Lips 1990). In addition, the solubilisation of cell wall polymeric material and softening

L. Day (✉) · M. Xu · S. K. Øiseth · Y. Hemar · L. Lundin
Food Futures Flagship, CSIRO Food and Nutritional Sciences,
671 Sneydes Road,
Werribee, Victoria 3030, Australia
e-mail: li.day@csiro.au

of cell walls as a function of temperature may also affect the viscosity and flow behaviour of the dispersion. Due to the irregular shape and the elasticity of the plant cell wall particles, they can interact at relatively low critical concentrations above which particle networks can be formed (Bayod et al. 2008). These networks show soft solid-like behaviour and exhibit a yield stress.

In this study, the effect of a range of thermal and mechanical processes on the creation of plant particle dispersions was investigated. The morphology of the plant particles was studied using confocal laser scanning microscopy. The viscoelastic properties and flow properties of the resulting dispersions were determined and related to the differences in particle morphologies.

Materials and Methods

Preparation of Carrot Cell Wall Particle Dispersions

Carrots (*Daucus carota*) were obtained from a local supermarket. Carrots were peeled and cut into approx. 2-cm pieces long cylinders along the length of the carrot root. The top and bottom end parts of the carrots were discarded, and the cylinder pieces were further cut into quarters. Water (200 g) was pre-heated to 80 °C or 100 °C. Carrot pieces (200 g) were added to the pre-heated water and heated at 80 °C for 10 min (blanched) or 100 °C for 30 min (cooked), followed by immediate cooling on an ice bath for 10 min. After cooling, additional deionised water was added to make up for the evaporated amount. The blanched or cooked carrots, plus the water, were then transferred to a kitchen blender (Philips Blender HR 2835 400 W) and blended for a total of 8 min to create dispersions containing primarily ‘cluster-cells’ (from the blanched carrots) or ‘single cells’ (from the cooked carrots). The ‘cell-fragment’ dispersion was prepared by further shearing of the cooked blended carrot dispersion. Sodium azide (0.01 wt.%) was added to the dispersions to prevent microbial growth during the 1 week analysis period.

Particle Size Distribution

Apparent particle size distribution was measured by laser light scattering using a Malvern Mastersizer 2000 instrument (Malvern Instruments Ltd, Worcestershire, UK). A refractive index of 1.560 for the cell wall particles, absorption of 0.1 for the dispersion and a refractive index of 1.33 for water were used as the optical properties of the dispersion. The particle calculation was set for irregular particles. Volume median diameter value $d(0.5)$ was used as the average particle size. Each sample was measured in duplicate, and results were within 1% variation.

Confocal Laser Scanning Microscopy

Confocal laser scanning microscopy (CLSM) was used to characterise the microstructure of the particles. Particle dispersions were diluted with deionised water to various degrees to refrain from imaging close-packed particles. Samples were stained with the fluorescent dye Congo red (0.005%), then observed under a HC PL APO $\times 20$ or a HCX PL APO $\times 63$ objective using a Leica TCS SP5 confocal laser scanning microscope (Leica Microsystems, Wetzlar, Germany) at room temperature. The fluorescent dye was excited by an Argon 488-nm laser, and the emitted light was collected at 544–663 nm. The examination depth varied from about 10 to 80 μm over the range of visualised areas and samples.

Total Solid Content

The total solid content of the dispersions was determined in duplicate according to the AOAC Official Method 964.22. About 15 g (one tablespoon) of washed sand was added to a flat bottom metal dish and dried at 102 °C for a minimum of 30 min. The dish was then allowed to cool down in a desiccator before the sample (about 10-g dispersion) was added to each dish and mixed using a glass rod to ensure an even distribution of the sample over the base of the dish. A small amount of deionised water was added if the sample was difficult to mix. The dish was then placed in a boiling water bath to remove most of the moisture, followed by drying in a 70 °C vacuum oven for 2–3 h with a dry air flow (through silica gel) at a maximum pressure of 700 mbar. After drying, the dish was transferred to a desiccator and weighed as soon as the sample reached room temperature to minimise moisture uptake. Two replicates of each sample were analysed.

Rheology Measurements

The rheological measurements on the dispersions were performed using a Paar Physica controlled-stress rheometer (Model MCR 300, PHYSICA Meßtechnik GmbH, Stuttgart, Germany) at 25 °C. Frequency sweep measurements (0.01–10 Hz) were carried out at a constant strain of 0.1% and strain sweep measurements at a constant frequency of 0.1 Hz using double-gap geometry. Flow curves were obtained using vane geometry under the controlled shear stress mode. The sample was allowed to rest for 10 min after loading prior to the test, and the sample cell was covered throughout the test. The data collection was set to ten points/decade in log scale for frequency, strain and shear stress, respectively. Dispersions were prepared from two different batches of raw carrots, and duplicate measurements were carried on each sample.

Results and Discussion

Effect of Processing on Particle Structure

Figure 1 CLSM images show the effects of heat treatment on carrot plant cell wall microstructure and particle morphologies of the dispersions produced using shear processes from raw and heat-treated carrot pieces. Heating up to 80 °C caused partial detachment between the cell walls (Fig. 1b), due to the solubilisation of pectin in the middle lamellae (Sila et al. 2005). By applying more severe heat treatment (cooking at 100 °C), clear separation of individual cells was observed as a result of the loss of most of the intercellular connection through pectin molecular interactions (Fig. 1c). The heat treatments also caused the loss of turgor pressure.

When mechanical shear force was applied to the plant tissues, the resulting particle microstructure and size depended on the microstructure of the start material. Without heat treatment, a particle dispersion of cell wall clusters with an average particle size ($d(0.5)$) of about 230 μm , was produced using a kitchen blender. The particles varied in size and shape, but all had a very rough surface with protruding plant cell wall fragments originating from the physical tearing of the cell walls during shear (Fig. 1d). With mild temperature treatment (e.g., 80 °C for 10 min), subsequent shear processing using the kitchen blender produced a particle dispersion with the particle morphology similar to the dispersion produced from the raw carrot pieces, only lightly smaller particle sizes (d

(0.5) = ~200 μm). The dispersion was made up primarily of cell clusters (Fig. 1e). This suggests that the detachment of cell wall between the lamellae was still strong enough to prevent cell separation. Cell wall structure was broken up to random cell wall clusters causing partial detachment between the cell walls.

On the other hand, when mechanical force was applied to the cooked tissues, a particle dispersion primarily consisting of single cells ($d(0.5)$ = ~70 μm) was obtained (Fig. 1f). This suggests that heating at 100 °C for 30 min caused sufficient solubilisation of pectins in the lamellae, which allowed cells to be separated easily when the shear force was applied. The surface of these particles was smoother, since the cell walls remained intact.

Further shear processing using a high shear homogeniser caused further breakdown of the cell clusters or single cells into irregular cell wall fragments ($d(0.5)$ = ~30 μm) with no distinctive cell structure (Fig. 1g).

The results showed that the particle morphology of plant dispersions can be controlled by the application of different heat treatment and shear forces.

Viscoelastic Properties of Carrot Cell Wall Particle Dispersions

Figure 2 shows the frequency dependency of the storage modulus (G') and the loss modulus (G'') at various total solids content for the 'cluster-cell' dispersion produced by blending the blanched carrot tissues and the 'single-cell' dispersion produced by blending the cooked carrot tissues.

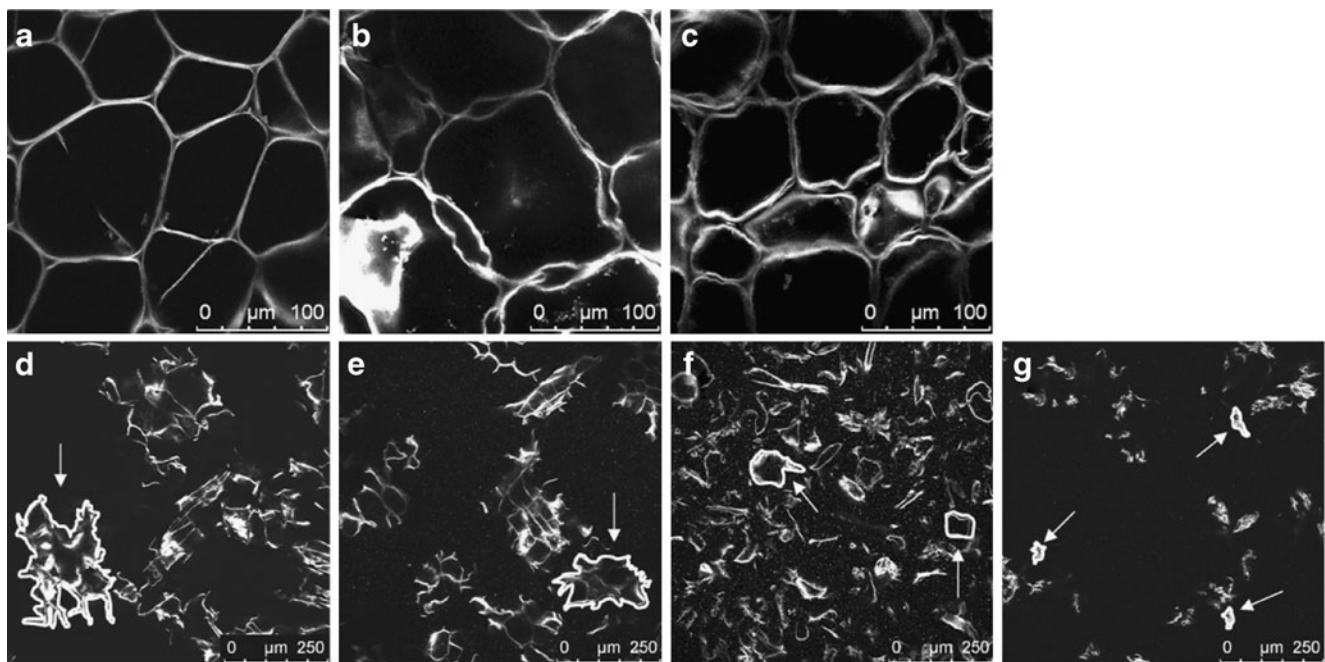


Fig. 1 CLSM images of carrot tissues and suspensions; **a** raw tissue, **b** blanched (80 °C, 10 min) tissue, **c** cooked (100 °C, 30 min) tissue, **d** cell wall particle dispersion produced from raw tissue by blending, **e** cluster-cell dispersion from blanched tissue, **f** single-cell dispersion

from cooked tissue and **g** cell-fragment dispersion from cooked tissue. The shapes of particles have been highlighted in images **d–g** by the addition of *white contours* and *arrows*

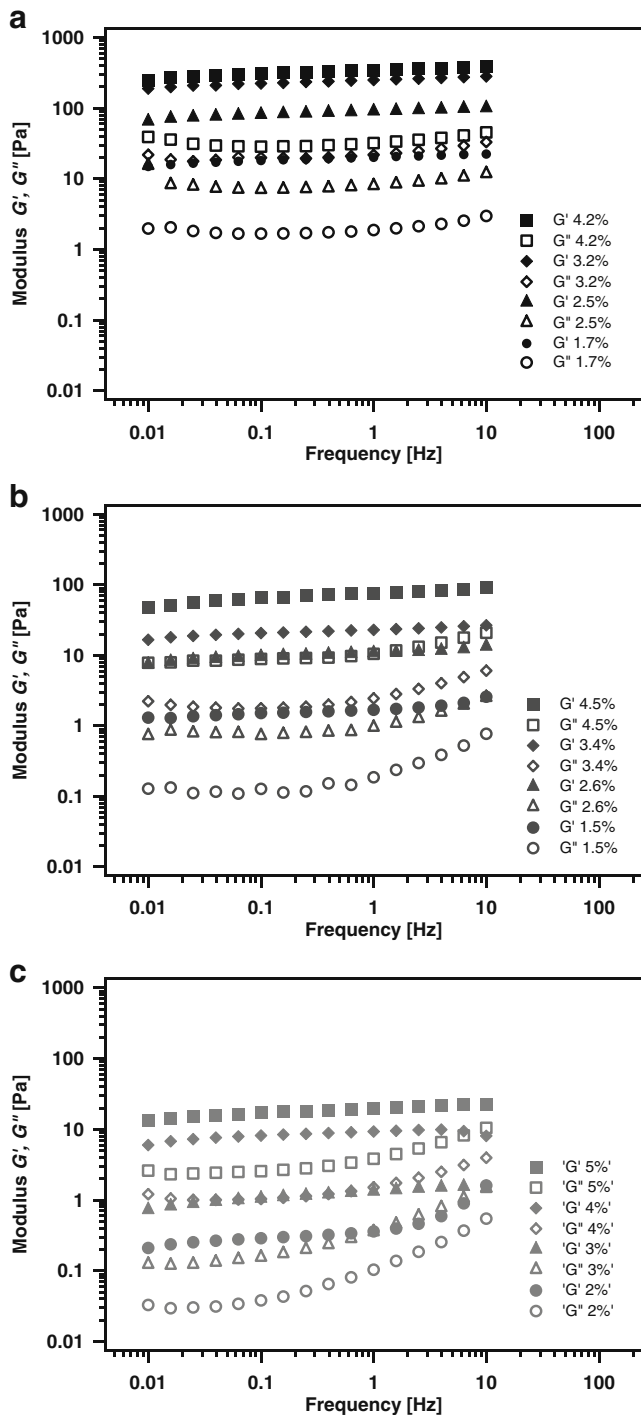


Fig. 2 Frequency dependence of the storage modulus G' (solid symbols) and loss modulus G'' (open symbols) for the plant cell dispersions of different solid concentrations: **a** ‘cluster-cell’ particle dispersion prepared by heat treatment of carrot tissues at 80 °C for 10 min followed by homogenisation using the kitchen blending; **b** ‘single-cell’ particle dispersion prepared by heat treatment of carrot tissues at 100 °C for 30 min followed by homogenisation same as **a**; and **c** ‘cell-fragment’ particle dispersion, prepared by further high shear homogenisation of **b**

The results showed that the dispersions behaved like a weak gel as G' was greater than G'' by less than a decade (Clark and Ross-Murphy 1987), and G' increased slightly with the increase in frequency for all three particle dispersions over a wide range of solids concentration.

Figure 3 shows the storage modulus G' and loss modulus G'' for the ‘cluster-cell’, ‘single-cell’ and ‘cell-fragment’ dispersions as a function of strain, at a similar solid content of ~2.5%. The linear viscoelastic region, where G' and G'' are independent of the applied strain is narrow, between approx. 0.05 and 0.5%. Qualitatively, the results were similar to that reported in literature for rehydrated apple and carrot cell wall (Vetter and Kunzek 2003; Schalow and Kunzek 2004; Pickardt et al. 2004). However in the present work, a much wider range of solids concentration was investigated and demonstrated that cell wall particle dispersions showed weak gel-like rheological behaviour even at low solid concentration (1 to 2%). At a similar total solid content, both storage modulus G' and loss modulus G'' were highest for the ‘cluster-cell’ dispersion, followed by the ‘single-cell’ dispersion, and lowest for the ‘cell-fragment’ dispersion. This suggests that, at the same total solid content, the ‘cluster-cell’ particles formed a more rigid network, than the ‘single-cell’ and the ‘cell-fragment’ particles.

In order to further understand the nature of particle interaction and network properties, the storage moduli G' at 0.1% strain (within the linear viscoelastic region) as a function of total solids (TS) for the particle dispersions with the three different particle morphologies were plotted (Fig. 4).

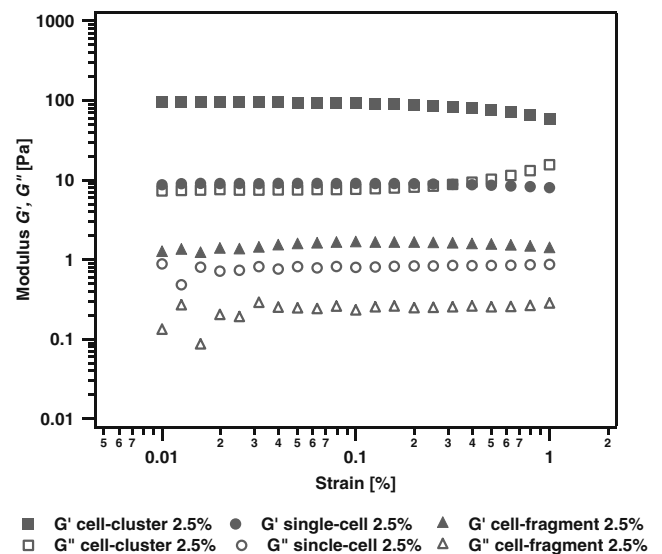


Fig. 3 Strain dependence of the storage modulus G' (solid symbols) and loss modulus G'' (open symbols) for the plant cell dispersions at ~2.5% solid content. ‘Cluster-cell’ and ‘single-cell’ dispersions prepared by heat treatment of carrot tissues at 80 °C for 10 min or 100 °C for 30 min, respectively followed by homogenisation using the kitchen blending; and ‘cell-fragment’ dispersion prepared by further high shear homogenisation of ‘single-cell’ dispersion

Due to the difficulties in accurately determining the phase volume of plant cell wall particles because of the compressible and fragile nature of the soft solid particles, the mass fraction of solids (e.g., the total solids) was used instead to model the rheological behaviour of the particle dispersions.

The rheological behaviour exhibited three regions for the ‘cluster-cell’ and ‘single-cell’ particle dispersions can be separated into three regions, while for the ‘cell-fragment’ dispersion, two regions were identified. In the first dilute and semi-dilute region (I) where the particle solids concentration were lower than 1% for the ‘cluster-cell’ and ‘single-cell’ dispersions, and less than 2% for the ‘cell-fragment’ dispersion, the G' scales linearly with TS . In this region where the particles have limited contact, the measurement is largely dominated by the volume occupied by the individual particles. The increase of G' is in proportion with the increase in total particle content.

In the second solids concentration region (II), G' shows a power-law relationship to TS in the form TS^α , with $\alpha=6.3\pm 0.5$ for ‘cluster-cell’, $\alpha=3.0\pm 0.2$ for ‘single-cell’ and $\alpha=3.9\pm 0.2$ for ‘cell-fragment’ dispersions, respectively. With the increase in the total particle content, the particles start to form networks, since the particles are close enough to touch each other, resulting in a sharp increase of the G' —two orders of magnitude in the case of ‘cluster-cell’, when total solids content was increased from 1 to 2%. The ‘cluster-cell’ and ‘single-cell’ particles interact with one another at a lower total solids content (1%) than the ‘cell-fragment’ particles (starting from 2%). This difference in the rheological behaviour is due to the difference in the size and morphologies of the particles.

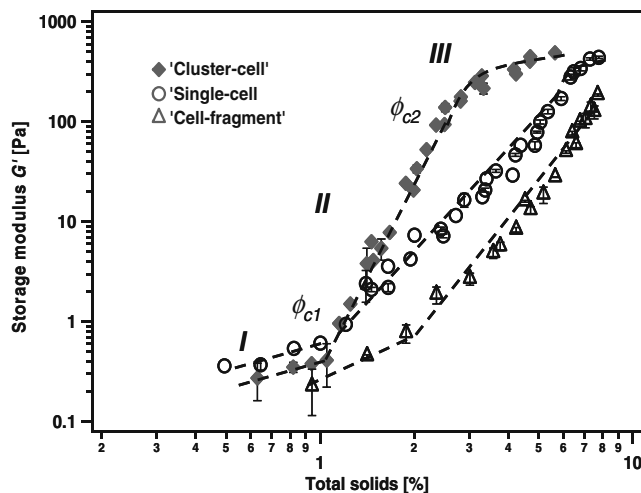


Fig. 4 Storage modulus G' at 0.1% strain and 1-Hz frequency, as a function of total solid for carrot cell wall particle dispersions containing ‘cluster-cell’ or ‘single-cell’, prepared by heat treatment of carrot tissues at 80 °C for 10 min or 100 °C for 30 min, respectively followed by homogenisation using the kitchen blending; or ‘cell-fragment’ dispersion prepared by further high shear homogenisation of ‘single-cell’ dispersion. Error bars represent standard deviations. Lines are: (I) linear plot; (II) power law equation and (III) Eq. 1 (see text for further details)

Finally, in the case of ‘cluster-cell’ and ‘single-cell’ particles, a third (III) region was observed where the total solids content was above approx. 3% for ‘cluster-cell’ and 6% for ‘single-cell’ dispersion. This is probably due to the particles ability to pack at a concentration higher than the critical close-packed concentration (Adams et al. 2004; Pabst et al. 2006) because the particles are soft and can deform. At very high total solids content, both dispersions are effectively above close-packed particles and have similar modulus values at their plateau. This indicates that the elasticity of the individual particles for both dispersions is within the same order of magnitude. If the individual particle elasticity differed, then a different plateau G' at high solids concentrations would be expected (Stokes and Frith 2008). In other words, upon concentration, the original dispersed particles, single cells or cell clusters, are brought closer to each other to constitute a continuous phase made of cells having the same elasticity. In this region, the particles are believed to be deformed, and the curved rheological behaviour could be modelled using a simple equation (Adams et al. 2004):

$$G' = A \left[1 - \left(\frac{\varphi_{c2}}{\varphi} \right)^{1/3} \right] \quad (1)$$

Where A is an adjustable parameter and φ is the total solids content and φ_{c2} is the critical TS content at which the particles are close packed. Fitting the experimental data using Eq. 1 and the software OriginPro8 yields $A=3,228\pm 286$ Pa and $\varphi_{c2}=0.049\pm 0.002$ for the ‘single-cell’ dispersion and $A=1,667\pm 88$ Pa and $\varphi_{c2}=0.020\pm 0.001$ for the ‘cluster-cell’ dispersion (Fig. 4). To the best of our knowledge, this is the first time that a model developed for soft-gel particles was successfully applied to describe the behaviour of cell wall particles when their concentration exceeds that corresponding to the critical packing volume.

Flow Behaviour and Yield Stress

Rotating vane geometry has been used to measure the flow properties and the yield stress of structured plant particle dispersions (Barnes and Carnali 1990; Barnes and Nguyen 2001; Stokes and Telford 2004). The methods have been used to study the rheological properties of starch granule dispersions and other concentrated food material made of particle dispersions (Genovese and Rao 2005; Tattiyakul et al. 2009). The advantage of using the vane geometry is that the insertion of the vane into the sample cup causes minimum structural disruption to the sample.

Figure 5 shows the apparent viscosity as function of the applied shear stress for the ‘cluster-cell’ and ‘single-cell’ dispersions at various solid concentrations. The dispersions exhibited typical structured fluid behaviour, with an abrupt transition from very high viscosity ($>10^4$ Pa s) to low-viscosity liquid (~ 1 Pa s) (Stokes and Telford 2004; Genovese and Rao

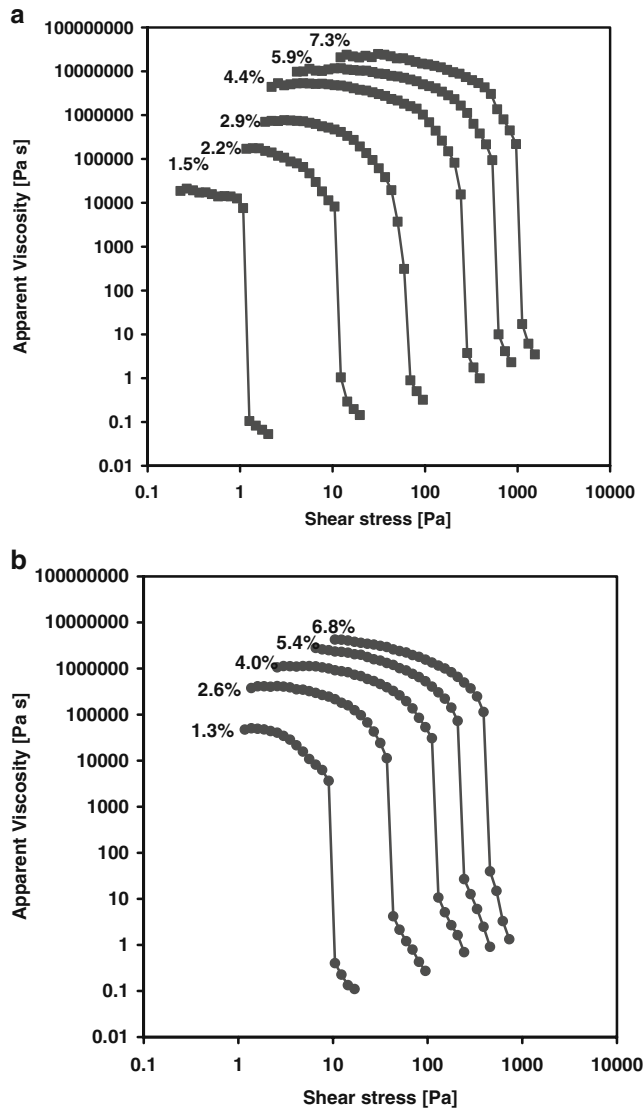


Fig. 5 Apparent viscosity for **a** ‘cluster-cell’ dispersion; **b** ‘single-cell’ dispersion, measured as a function of shear stress, showing increased yield stress as a function of total solid. The dispersions were prepared by heat treatment of carrot tissues at 80 °C for 10 min or 100 °C for 30 min respectively, followed by homogenisation using the kitchen blending

2005). The yield stress (σ_y) is here defined as the stress at which this transition in viscosity occurs. For example, $\sigma_y = 10$ Pa for the 2.2% dispersion of ‘cluster-cell’ (see Fig. 5a). Studies have shown that the yield stress could be obtained by modelling the vane geometry measurements by the Cross model, the Herschel–Buskley model (Stokes and Telford 2004) or the Casson model (Missaire et al. 1990). When the applied stress is less than σ_y , the dispersion does not flow but deforms plastically like a solid, with definite strain recovery upon the removal of the stress. When the σ_y is exceeded, the dispersion flows like a truly viscous material with finite viscosity. This behaviour was observed at a wide range of solid contents above the concentration (φ_{c1}) where the particle network started to form.

The yield stress σ_y (the minimum stress required to enable the flow) as a function of total solid content for the ‘cluster-cell’ and ‘single-cell’ dispersions is shown in Fig. 6. For both dispersions and over three decades in σ_y , the Log of σ_y increased linearly with the Log of total solids content. However the rate of increase of σ_y for the ‘cell cluster’ dispersion was faster than that of ‘single-cell’ dispersions; i.e., a slope of ~ 4.2 and ~ 2.2 were calculated for the ‘cluster-cell’ and ‘single-cell’ dispersions, respectively (see Fig. 6). Furthermore, at low total solids content ($<4\%$) σ_y of the ‘single-cell’ dispersions was higher than that of the ‘cluster-cell’ while at higher total solid contents ($>4\%$) σ_y of the ‘cluster-cell’ dispersions was higher than that of the ‘single-cell’. This could be explained as follow: at low total solids content, the yield stress is due to the jamming (restricted movement) of the cell wall particles, and at high concentrations the yield stress is due to the fact that the particles are highly packed. It is expected that the ‘single-cell’ particles will jam at low concentration, since they appear more elongated (Fig. 1g) than the ‘cluster-cell’ particles (Fig. 1e) and for the same total solids content, ‘single-cell’ particles occupy a larger effective phase volume than the ‘cluster-cell’ particles, since the later is made by a collection of tightly packed single cells. Inversely, at high total solids content, both the ‘single-cell’ and ‘cluster-cell’ particles in the dispersion are highly close-packed; σ_y will be less affected by the morphology (elongation against sphericity) of the particles. At these high total solid concentrations, they behave similarly to that of highly concentrated elastic droplets (Mason et al. 1995), where it is expected that

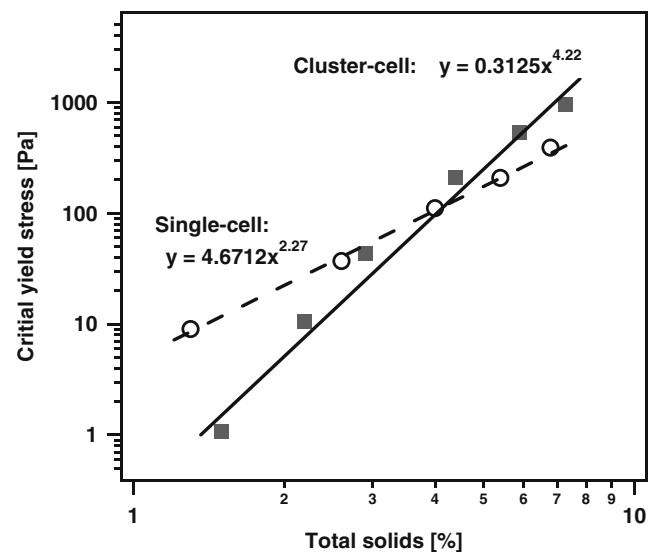


Fig. 6 Log–log plot of the yield stress vs. total solid contents for dispersions made of ‘cluster-cell’ and ‘single-cell’ dispersions. The dispersions were prepared by heat treatment of carrot tissues at 80 °C for 10 min or 100 °C for 30 min respectively, followed by homogenisation using the kitchen blending

σ_y will depend on the size, the deformability and the entanglement behaviour of these particles. In this case, the ‘cluster-cell’ particles are expected to be more deformable, due to their cellular structure, and to entangle more because of the rough surface caused by the protruding plant cell wall fragments. Linear relationships between the yield stress and pulp content for apple sauce and tomato concentrates have been reported (Yoo and Rao 1994). This is likely due to the difference in the range of particle solid concentration examined. The pulp concentration examined by Yoo and Rao (1994) (pulp content greater than 20%) was much higher than the highest concentration used in this study, and likely to exceed the concentration at which particle full packing is achieved.

Conclusions

Using a combination of heat and shear processes, plant tissues can be comminuted to plant cell wall particles of different firmness, sizes and shapes to impart a range of different textures, ranging from flowable, spoonable to paste-like. The cell wall particle dispersions showed typical structured fluid behaviour with the storage modulus G' greater than the loss modulus G'' in the linear viscoelastic range with only a slight dependence of the moduli on frequency even at a low solids concentration (e.g., ~1%). The particles interact to form a gel-like network resulting in a steep increase in their moduli at a relatively narrow solid concentration range, which is dependent on the particle size and shape of the dispersions. In addition, the particle dispersions showed that the viscosity decreased sharply from a high zero-shear viscosity to a viscosity several decades lower after a yield stress is reached. This yield stress was also dependent on the size and shape of the cell wall particles. Although these findings are obtained on carrot cell wall particles, other plants such as broccoli could be also utilised as a starting material to produce particles with similar rheological behaviour. This work demonstrates that different morphological and rheological properties of plant-based materials could be used to control product texture and to increase the levels of dietary fibre (1.5–3%) that could have physiological impact (Redgwell and Fischer 2005; Rodríguez et al. 2006).

References

- Adams, S., Frith, W. J., & Stokes, J. R. (2004). Influence of particle modulus on the rheological properties of agar microgel suspensions. *Journal of Rheology*, *48*, 1195–1213.
- Barnes, H. A., & Carnali, J. O. (1990). The vane-in-cup as a novel rheometer geometry for shear thinning and thixotropic materials. *Journal of Rheology*, *34*, 841–866.
- Barnes, H. A., & Nguyen, Q. D. (2001). Rotating vane rheometry—A review. *Journal of Non-Newtonian Fluid Mechanics*, *98*, 1–14.
- Bayod, E., Willers, E. P., & Tomberg, E. (2008). Rheological and structural characterization of tomato paste and its influence on the quality of ketchup. *LWT-Food Science and Technology*, *41*, 1289–1300.
- Clark, A., & Ross-Murphy, S. (1987). Structural and mechanical properties of biopolymer gels. *Biopolymers*, *57*–192.
- Di Giacomo, G., & Taglieri, L. (2009). A new high-yield process for the industrial production of carrot juice. *Food and Bioprocess Technology*, *2*, 441–446.
- Evans, I. D., & Lips, A. (1990). Concentration dependence of the linear elastic behaviour of model microgel dispersions. *Journal of the Chemical Society, Faraday Transactions*, *86*, 3413–3417.
- Genovese, D. B., & Rao, M. A. (2005). Components of vane yield stress of structured food dispersions. *Journal of Food Science*, *70*, E498–E504.
- Genovese, D. B., Lozano, J. E., & Rao, M. A. (2007). The rheology of colloidal and noncolloidal food dispersions. *Journal of Food Science*, *72*, R11–R20.
- Mason, T. G., Bibette, J., & Weitz, D. A. (1995). Elasticity of compressed emulsions. *Physical Review Letters*, *75*, 2051–2054.
- Missaire, F., Qiu, C.-G., & Rao, M. A. (1990). Yield stress of structured and unstructured food suspensions. *Journal of Texture Studies*, *21*, 470–490.
- Ortega-Rivas, E. (2009). Bulk properties of food particulate materials: an appraisal of their characterisation and relevance in processing. *Food and Bioprocess Technology*, *2*, 28–44.
- Pabst, W., Gregorova, E., & Berthold, C. (2006). Particle shape and suspension rheology of short-fiber systems. *Journal of the European Ceramic Society*, *26*, 149–160.
- Pickardt, C., Dongowski, G., & Kunzek, H. (2004). The influence of mechanical and enzymatic disintegration of carrots on the structure and properties of cell wall materials. *European Food Research and Technology*, *219*, 229–239.
- Redgwell, R. J., & Fischer, M. (2005). Dietary fiber as a versatile food component: An industrial perspective. *Molecular Nutrition & Food Research*, *49*, 521–535.
- Rodríguez, R., Jiménez, A., Fernández-Bolaños, J., Guillén, R., & Heredia, A. (2006). Dietary fibre from vegetable products as source of functional ingredients. *Trends in Food Science & Technology*, *17*, 3–15.
- Schalow, S., & Kunzek, H. (2004). The influence of predrying treatment and of suspension solution conditions on the rehydration of apple cell wall materials. *European Food Research and Technology*, *219*, 329–340.
- Sila, D. N., Smout, C., Vu, S. T., Van Loey, A., & Hendrickx, M. (2005). Influence of pretreatment conditions on the texture and cell wall components of carrots during thermal processing. *Journal of Food Science*, *70*, E85–E91.
- Stokes, J. R., & Telford, J. H. (2004). Measuring the yield behaviour of structured fluids. *Journal of Non-Newtonian Fluid Mechanics*, *124*, 137–146.
- Stokes, J. R., & Frith, W. J. (2008). Rheology of gelling and yielding soft matter systems. *Soft Matter*, *4*, 1133–1140.
- Tattiyakul, J., Liao, H. J., & Rao, M. A. (2009). Role of structure in the measurement of flow properties of food and starch dispersions: A review. *International Journal of Food Properties*, *12*, 2–10.
- Valencia, C., Sanchez, M. C., Ciruelos, A., Latorre, A., Madiedo, J. M., & Gallegos, C. (2003). Non-linear viscoelasticity modeling of tomato paste products. *Food Research International*, *36*, 911–919.
- Vetter, S., & Kunzek, H. (2003). The influence of the pre-drying treatment on the hydration properties of dried cell wall materials from apples. *European Food Research and Technology*, *216*, 129–137.
- Yoo, B., & Rao, M. A. (1994). Effect of unimodal particle-size and pulp content on rheological properties of tomato puree. *Journal of Texture Studies*, *25*, 421–436.